Numerical and Experimental Investigation of Bentonite-Sand Mixtures

Mahsa Shafaei Bajestani, Othman Nasir
Department of Civil Engineering – University of New Brunswick, Fredericton, New Brunswick, Canada

ABSTRACT
Deep geological repository (DGR) is the most preferred option for the long-term disposal of low, intermediate, and high-level radioactive wastes in many countries. DGR safety depends mainly on the multiple-barrier system of both natural and engineered barriers. Bentonite-based materials have been suggested as one of the effective engineering barriers in DGR, due to their low permeability, high swelling pressure, and retention of radionuclides. Swelling characteristics of bentonite-based materials is a crucial factor in assessing its long-term performance, hence the safety of DGR. Numerous laboratory tests have been conducted to determine the swelling properties of bentonite-based sealing materials. In this study, laboratory tests on swelling properties are performed using different standard methods such as the free swelling and constant volume methods. Additionally, numerically simulated swelling tests are conducted to predict swelling characteristics of bentonite-based material and compared with the experimental results.

RÉSUMÉ
Le dépôt dans des formations géologiques profondes (DFGP) est l'option la plus privilégiée pour l'entreposage à long terme des déchets radioactifs de faible, moyenne et haute activité dans de nombreux pays. La sécurité du DFGP dépend principalement du système à barrières multiples engendré tant naturellement que par une structure d'ingénierie. Les matériaux à base de bentonite ont été suggérés comme l'une des barrières d'ingénierie efficaces dans le DFGP, en raison de leur faible perméabilité, de leur pression de gonflement élevée et de leur rétention de radionucléides. Les caractéristiques de gonflement des matériaux à base de bentonite sont un facteur crucial dans l'évaluation de ses performances à long terme, d'où la sécurité du DFGP. De nombreux tests de laboratoire ont été effectués pour déterminer les propriétés de gonflement des matériaux d'étanchéité à base de bentonite. Dans cette étude, des tests de laboratoire sur les propriétés de gonflement ont été effectués en utilisant différentes méthodes standard telles que les méthodes de gonflement libre et de volume constant. De plus, des tests de gonflement simulés numériquement ont été effectués pour prédire les caractéristiques de gonflement du matériau à base de bentonite et comparés aux résultats expérimentaux.

1 INTRODUCTION

The preferred solution for the final storage of low, intermediate, and high-level radioactive waste (HLW) is the deep geological repository (DGR), which is being considered in several countries (Wang et al. 2012). The DGR consists of a multi-barrier system to support long-term containment and isolation of radioactive waste from the public and the environment. The multi-barrier system mainly includes the natural barrier system, which consists of the host rock and the engineered barrier system that consists of backfill, buffer/sealing materials, and waste canisters. Due to its low permeability and high swelling, bentonite and bentonite-based materials are selected as buffer/sealing materials in many DGR designs (Sun et al. 2015).

Following the closure of the DGR, the groundwater table is expected to rebound by infiltration from the host rock. Then, the hydration process begins, and the bentonite-based materials will swell due to wetting (Wang et al. 2012). Complete saturation of DGR requires almost 2,000 years (Briggs and Krol, 2018). One of the objectives of using materials that swell is to close technological voids created as a results of waste emplacement within the DGR. The performance of sealing materials experiencing swelling pressure, deformation, and volume change are major factors that can impact the stability of the DGR. Therefore, the swelling pressure should be high enough to support the long-term sealing properties, and moreover, the swelling pressure should not exceed the in-situ principal minor stress to ensure the mechanical stability of the DGR (Wang et al. 2012). Hence, the investigation of the swelling properties of bentonite-based materials during the hydration process is crucial to assess the safety of the whole repository system.

The chemical compositions of the hydration fluid influence the swelling process of bentonite-based materials. By increasing the salinity content of the porewater, the swelling capacity of bentonite decreases. Increasing porewater salinity reduces repulsive forces within the diffuse double of the mineralogical structure of bentonite and consequently diminishes its swelling

capacity. (Karnland and Muurinen, 2005; Komine et al. 2009; Wang et al. 2012; Zhu et al. 2013).

The swelling properties of various types of bentonite and its mixture with sand have been studied extensively. For instance, Wang et al. (2012); Sun et al. (2013); Sun and Fang (2014) have investigated the swelling characteristics of MX80 bentonite hydrated by utilizing distilled water and synthetic water, Gaomiaozi (GMZ) Na-bentonite saturated with distilled water, and GMZ Ca-bentonite inundated with distilled water, respectively. Two main conclusions may be drawn from their findings. First, swelling properties of different types of bentonite depend on the initial dry density of the sample. Increasing the initial dry density causes higher swelling pressure and swelling strains. Second, the effect of initial water content on swelling properties which does not have a great influence on the swelling pressure. Different studies were examined the swelling properties of different types of bentonite-based materials using different test methods including constant-volume method, pre-swell method, zero-swell method, and swell–consolidation method (Sun et al. 2015; Wang et al. 2012). Various experimental tests result in different values of swelling pressure because of different loading and wetting procedures (Zhu et al. 2013; Sun et al. 2015; Wang et al. 2012).

Safety and stability of the DGR system are controlled by different physical and chemical processes, such as heat transfer (Thermal process, T), flow (Hydraulic process H), stress-strain and deformation (Mechanical process, M), and solute transport and chemical reactions (Chemical process, C). The couplings among the T, H, M, and C processes or THMC coupled processes in the field of rock and soil mechanics have become important subjects since the 1980s. The term "coupled processes" implies that each process affects the initiation and progress of all other processes (Jing and Feng 2003). Thus, the response of a porous medium to radioactive waste storage cannot be predicted by considering each process individually or in direct succession. Changes in the system state variables (temperature, concentration, deformation, and pressure) through THMC processes are often calculated by solving partial differential equations (PDEs) derived to express THMC processes mathematically. The implementation of coupled processes in safety assessment became a critical requirement to ensure a better representation of the actual field conditions and adequate long-term analysis of the DGR. The focus of this study is on the HM behavior of bentonite-based materials that is an interaction between the flow and deformation of porous medium. H processes are described with fluid pressure, permeability, saturation, porosity, and density. M processes are defined by stress, deformability, displacement, and stiffness. The HM processes governing the hydration of bentonite in sealing systems are strongly coupled such that a change in its state of hydration causes a change in the effective stress which computed by the mechanical process. The DECOVALEX is an international research project that used experimental and field works to validate the developed coupled process mathematical equations and codes. Various conceptual models taking into account the HM processes have been developed to simulate the hydration and swelling pressure development in the sealing system of DGR (Jing and Feng, 2003; Millard et al. 2016; Thatcher et al. 2016; Nasir et. al 2017b).

In this study, experimental and numerical investigations on the swelling properties of bentonite-sand are performed with different dry density and different bentonite-sand mixture. The numerical work included the simulations of the free swelling using FLAC3D software (Itasca Consulting Group 2011).

2 MATERIALS, EQUIPMENT, AND METHODS

2.1 Materials

A commercial bentonite from Wyoming, USA (OPTA), was used in this study. Table 1 lists the physical properties of the bentonite. The grain size distribution of bentonite is shown in Figure 1 and is determined through a hydrometer analysis. The grain size distribution shows that 67% of the grains are smaller than 2 μm (clay fraction).

The grain size distribution of sand is determined by sieve analysis as shown in Figure. 1. The sieve analysis of the sand indicates a medium grain size distribution.

Table 1. Physical properties of bentonite

Properties	Value
Specific gravity of Bentonite	2.50
Liquid limit (%)	493
Plastic limit (%)	41
Plasticity index	452

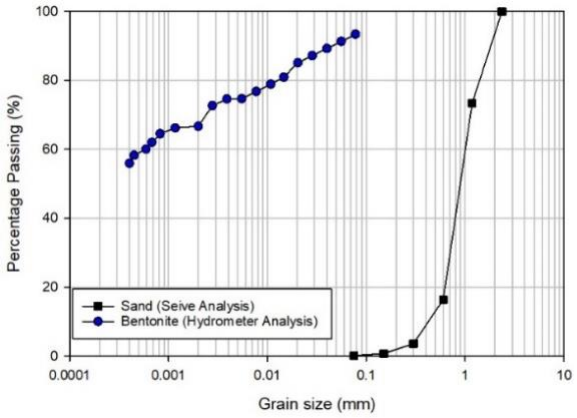

Figure 1. Grain size distribution of bentonite and sand

2.2 Equipment

A GDS dynamic triaxial (GDSDT) testing system is used in this study (GDS Instruments Ltd). The GDSDT is a 10 kN capacity triaxial self-control apparatus, based on an axially stiff load frame with an electro-mechanical actuator. GDSDT testing systems are commonly used to perform triaxial tests on a sample. For this study, the GDSDT is modified with a new extension pedestal to perform tests with an ELE fully confined oedometer cell. As a result, the modified GDSDT (MGDSDT) device, which presents in Figure 2, is capable to perform constant-volume (CV) and free swelling (FS) tests and measure the swelling pressure

and swelling strain of samples. For preparing compacted samples, an INSTRON Universal Testing System with 250 kN capacity, which is equipped to perform tensile, compression, bend, creep, and cyclic tests on all types of materials, is used to apply the compaction load.

2.3 Samples Preparation

In this study, testing was performed on samples of compacted bentonite (B100-Sa0) and bentonite-sand mixture (B70-Sa30) with a bentonite content of 70% in dry mass. Bentonite and sand particles were compacted under dry conditions.

Samples were statically compacted in an oedometer ring (50 mm in internal diameter and 19 mm height) at a controlled rate using an INSTRON Universal Testing System. After compaction, the specimen was carefully transferred into the oedometer cell, as shown in Figure 2, to perform the experiment.

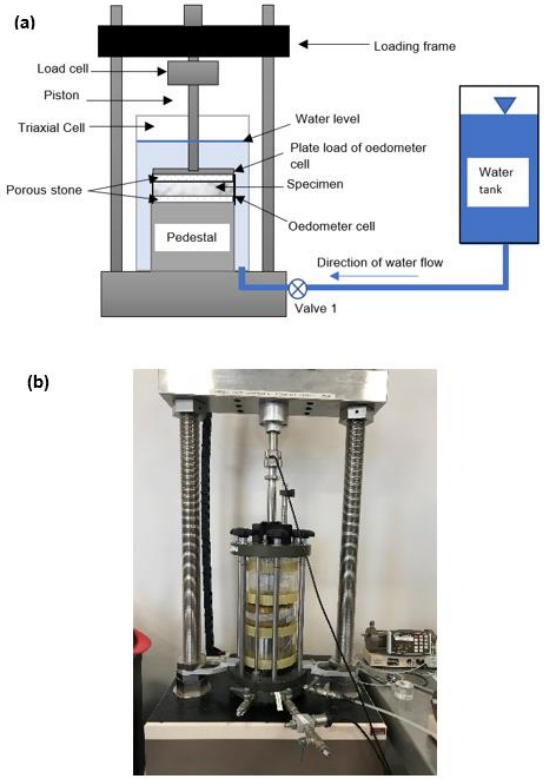

Figure 2. (a) Schematic view of MGDSDT, (b) MGDSDT device

2.4 Experimental Methods and Test Program

Series of constant-volume and free swelling tests were performed on the prepared bentonite and bentonite-sand mixture samples. The test program is summarized in Table 2. The test procedures are explained in the following sections.

Table 2. Test program

Test No.	Method	Final Dry Density[1] (g/cm3)
B70-Sa30-1.70	CV	1.70
B100-Sa0-1.70	CV	1.70
B70-Sa30-1.84	CV	1.84
B100-Sa0-1.84	CV	1.84
B100-Sa0-1.85	FS	1.85

[1]sample density is measured after finishing the test to get the final dry density

2.4.1 Constant-Volume Test

The constant-volume (CV) tests are mainly conducted based on the strained-controlled method. During the swelling process, the height of the sample increases due to saturation, and strain is defined as the change of height to the initial height of the sample. In CV tests, the expansive soil is prevented from further swelling strain through the hydration process by controlling the applied pressure, termed as swelling pressure. According to ASTM D4546-14. (2014) and Tang et al. (2011), two strained-controlled techniques can be used to perform the constant-volume method. The first technique includes applying a small load on the sample and then wetting the sample to start the swelling. Any swelling is prevented by incrementally increasing the load. When the vertical expansion approaches zero, the swelling pressure is defined as the total pressure applied to the sample. The second technique is the measurement of the swelling pressure by preventing the vertical swelling using a rigid reaction frame with a force transducer. The swelling pressure is achieved when the load cell approaches a constant value. In this study, the second technique is used.

The following steps are used to perform the CV tests using the MGDSDT device:

Step 1: Placing the odometer cell in the triaxial device.

Step 2: Setting up the device by applying initial vertical pressure and restricting the displacement.

Step 3: Opening valve 1 to supply de-aired distilled water and allowing it to reach the desired water level to start the wetting process as shown in Figure 2.

Step 4: Running the software to monitor the data and record the swelling pressure readings using the data acquisition system.

Step 5: Terminating the test after reaching a steady-state condition and constant swelling pressure.

All tests are carried out at constant room temperature. The full saturation and swelling have been indicated in all the tests when the swelling pressure has attained equilibrium. Full saturation is confirmed by measuring the sample saturation after finishing the experiment.

2.4.2 Free Swelling Test

The free swelling (FS) is defined as the free increase in soil volume due to the wetting under constant vertical pressure. The FS test is performed on pure bentonite with a dry

density of 1.85 g/cm^3. A sample of 5 mm in height is considered to provide sufficient space for swelling within the oedometer ring (19 mm height) for free swelling of bentonite as shown in Figure 2.

The procedure of performing FS test includes the following steps:

Step 1: Placing the odometer cell in the triaxial device.

Step 2: Setting up the device and allowing the displacement to change freely by keeping the applied load constant.

Step 3: Opening valve 1 to supply de-aired distilled water and allow the water to reach the desired water level and start the wetting process as shown in Figure 2.

Step 4: Running the software to monitor data and record the vertical displacement readings using the data acquisition system.

Step 5: Terminating the test after reaching steady-state condition and constant swelling strain.

In this study, the free swelling is performed on B100-Sa0-1.85 sample under a vertical pressure of 26 kPa, including the weights of the load plate and porous stones of the oedometer cell. The results of the FS test are used to obtain the required parameters for the swell model explained later in Section 3.

2.4.2.1 Free Swell Index

In addition to CV and FS tests, the free swell index test is one of the common simple tests to estimate the swelling potential of soil. This test is conducted by pouring 10 cm^3 of dry soil into a 100 mL jar filled with water and then measuring the swelled volume of soil after reaching constant value. The free swell test has some uncertainties, such as the difficulty of measuring the exact volume of 10 cm^3. The differential free swell is suggested to increase the accuracy of the test. The differential free swell test is performed by considering two samples of 10 g of oven-dried soil passing the 425 µm sieve. It should be noted that for material with high swelling potential such as bentonite, the weight of the dry soil sample is recommended to only 3 g. The first specimen poured into a 100 mL graduated jar filled with kerosene (a non-polar liquid that does not cause swelling of soil), and the second specimen is poured with distilled water. The final volume of both samples is recorded after 24 h (Sivapullaiah et al. 1987). The differential free swell index is given by Eq. 1:

$$\frac{V_d - V_s}{V_d} \times 100 \qquad [1]$$

where:

V_d =the volume of the sample contains distilled water and

V_s =the volume of the sample contains kerosene.

The objective of this test is to preliminarily confirm the swelling potential of the used bentonite.

3 NUMERICAL SIMULATION

3.1 Mathematical Model

3.1.1 Flow Model

Fluid mass balance is one of the fundamental conservation equations that can be expressed for small deformations and is included in FLAC3D as follows:

$$-q_i + q_v = \frac{\partial \zeta}{\partial t} \qquad [2]$$

where q_v is the volumetric fluid source intensity in [1/sec], and ζ is the variation of fluid content or variation of fluid volume per unit volume of a porous material due to diffusive fluid mass transport, q_i is the specific discharge vector that is described by Darcy's law as the fluid transport:

$$q_i = -k_{il}\hat{k}(s)\frac{\partial}{\partial x_l}(p - \rho_f x_j g_j) \qquad [3]$$

where k is the tensor of absolute mobility coefficients (FLAC3D permeability tensor that is defined as the ratio of intrinsic permeability to dynamic viscosity), k(s) is the relative mobility coefficient, which is a function of fluid saturation (s), p is fluid pore pressure, ρ_f is the fluid density, and x_j is the direction vector of gravity (g_j).

In the FLAC3D formulation, the influence of capillary pressure is neglected, and the fluid pressure is taken as zero when saturation is less than one. In order to represent the transition between saturated and unsaturated zones, a simple law that relates the relative permeability to the saturation by a cubic law was used. The relative permeability is zero for zero saturation and one for full saturation:

$$\hat{k}(s_{in}) = s_{in}^{\,2}(3 - 2s_{in}) \qquad [4]$$

where s_{in} is the average saturation at the inflow node. In addition to Eq. 4, the gravity term of Eq. 3 (i.e., ρ_f, x_j, g_j) is multiplied by the average zone saturation.

The fluid flow in swelling soil depends on the hydraulic parameters, especially permeability. Changes in porosity and pore size distribution cause the swelling properties of bentonite to be not constant and related to variables such as saturation and confining pressure (Nasir et al., 2017a). The model presented by Nasir et al. (2017a) predicted the changes of permeability of bentonite during the hydration process. In this study to simulate the FS test, the unsaturated formulation of FLAC3D and Nasir et al. (2017a) model are used. First, an initial saturated permeability is assigned to the model, then an additional parameter S_w is added to update the saturated permeability during the saturation. This parameter is a function of degree of saturation from 0.06 to 1.

3.1.2 Mechanical Model

Mechanical models describe the relationship between stress state and the resulting strains. The mechanical models available in FLAC3D range from linearly elastic models to highly nonlinear plastic models. Although soil is not completely linearly elastic, a linear elastic model can be utilized to describe the simplest representation of soil behavior in different geotechnical applications. Based on the linear and reversible Hooke's law, the strain increments generate stress increments by the following equation:

$$\Delta\sigma_{xx} = 2G\ \varepsilon_{xx} + \alpha_2(\varepsilon_{yy} + \varepsilon_{zz})$$
$$\Delta\sigma_{yy} = 2G\ \varepsilon_{yy} + \alpha_2(\varepsilon_{xx} + \varepsilon_{zz}) \quad [5]$$
$$\Delta\sigma_{zz} = 2G\ \varepsilon_{zz} + \alpha_2(\varepsilon_{xx} + \varepsilon_{yy})$$

where, $\alpha_2 = K - \frac{2}{3}G$

K and G are the bulk and shear modulus of soil, respectively.

In order to investigate the swelling process from a HM perspective using FLAC3D, a swelling model developed by Noorany et al. (1999) is used in this study. Noorany et al. (1999) studied wetting-induced deformations in swelling soil employing an elastic wetting model, which is referred to as the "swell model" (SM). The SM is one of the available mechanical constitutive models in FLAC 3D that requires a set of material parameters including a_1, c_1, a_3, c_3, and N_S. The mentioned parameters can be obtained experimentally on an isotopically loaded triaxial sample of swelling soil with a desired dry density and moisture content under various confining stress levels of laboratory testing as suggested by Noorany et al. (1999).

According to the experimental results obtained by Noorany et al. (1999), the wetting-induced strains can be expressed by either logarithmic or linear functions (the linear function is shown in Equation 6) in terms of vertical stress in the direction of swelling, σ_{zz}, normalized by atmospheric pressure, p_a:

$$\varepsilon_{zz} = c_1 - a_1(\sigma_{zz} / p_a)$$
$$\varepsilon_{xx} = \varepsilon_{yy} = c_3 - a_3(\sigma_{zz} / p_a) \quad [6]$$

In the above equations, ε_{zz} is the vertical wetting-induced strain in the direction of swelling, and the wetting strain is assumed to be isotropic in the lateral direction, i.e., $\varepsilon_{xx} = \varepsilon_{yy}$. It should be noted that the vertical stress component, σ_{zz}, is the vertical stress prior to wetting and is not modified in Eq. 6 during the calculation.

In order to implement the swell model in numerical analysis, the wetting-induce strains are estimated by Eq. 6 based on the first stress equilibrium condition. Then, the corresponding wetting stresses are derived based on the incremental form of Hooke's Law (Eq. 5). The calculated wetting stresses are added to the initial stresses, and the system is cycled until reaching the equilibrium that provides steady-state stress and displacements induced by wetting.

The SM developed by Noorany et al. (1999) does not consider saturation and time as part of the swelling processes, instead, the total swelling was divided into stages and implemented in the steps (N_s). In this work, we modified the SM to be time, and saturation dependent by an indirect approach. Hence, this constitutive model was modified to estimate swelling using an indirect coupling. The indirect coupling included the evaluating the saturation using the flow model, dividing the geometry into a smaller segment based on the saturation history. Different N_s swell model parameters then assigned to each segment to reach full swelling.

3.2 Material Properties of the Simulated Model

The SM parameters are obtained from the results of CV and FS tests on B100-Sa0 with a density of 1.85 g/cm^3. The linear variation of wetting strain to the vertical stress is plotted in Figure 3, using two data points obtained from CV and FS tests. By considering the linear equation explained in Section 3.1.2 (Eq. 6), the parameters are evaluated and summarized in Table 3. It should be noted that for the purpose of numerical simulation, the swelling case of the present study can be considered as a one-dimensional swell due to the confining boundaries on the sample provided by the oedometer ring, which prevents deformation in the horizontal direction, and therefore the parameter c_3 can be set to zero and a_3 is irrelevant.

Other properties, such as bulk, shear modulus, and initial saturated permeability are calibrated according to the experimental results and listed in Table 3.

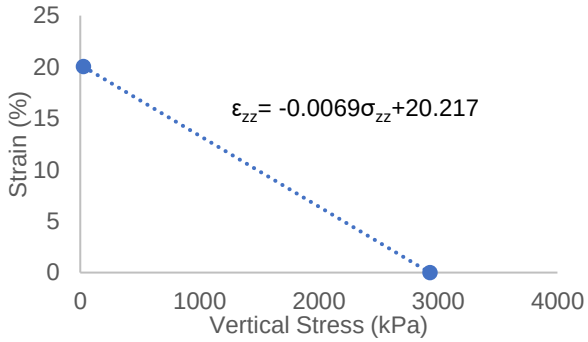

Figure 3. Swelling data from constant-volume and free swelling method (B100-Sa0-1.85)

Table 3- Parameters of the swell model (B100-Sa0-1.85)

Parameters	Value
Dry Density (gr/cm^3)	1.85
K (MPa)	32
G (MPa)	0.5
Initial Saturated permeability (m/s)	2×10^{-11}
a_1	0.0069
c_1	0.20217
a_3	irrelevant
c_3	0
N_s	Step varies depending on the segments

3.3 Geometry, Initial, and Boundary Condition

The simulated geometry is a one-dimensional vertical column model of a cubic block with an aspect ratio (length to width) of 1 for each zone. An aspect of one is adopted to reduce the solving time. The height of the sample is considered 5 mm to simulate the free swelling test. The mechanical boundary conditions are set as the following: all vertical faces of geometry are supported by rollers to allow vertical displacement without lateral movement. Moreover, the base is also supported by rollers and the

initial vertical pressure of 26 kPa is applied to the top of the sample.

The hydraulic boundary conditions are set as no flow from all sides and constant pressure of zero at the top and bottom. The constant zero pressure simulates free water supply from the top and bottom of the specimen. Figure 4 shows the geometry of the model and the boundary conditions of the numerical model.

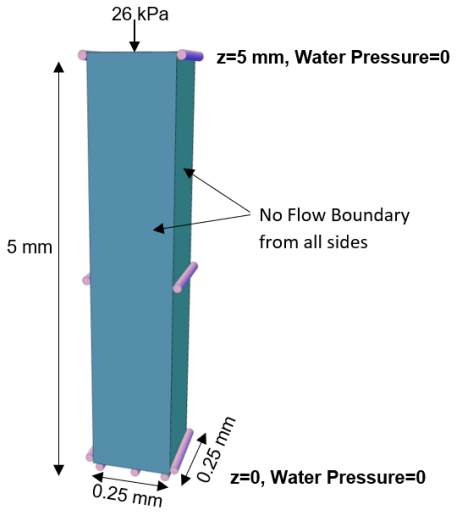

Figure 4. Conceptual representation of the simulation model

4 RESULT AND DISCUSSION

4.1 Experimental Results

4.1.1 Results of Constant-Volume (CV) Test

The results of swelling pressure versus time for different dry densities are presented in Figure 5. The evolution of swelling pressure during the hydration process shows a specific pattern for all different densities, in which, at the early stage, the swelling pressure increases up to a maximum value, subsequently drops and then start to gain, increasing until it finally reaches a steady-state and constant amount of swelling pressure. The reason for the mentioned behavior of the evolution pattern of swelling pressure can be explained by the structure of compacted bentonite (Push 1982; Komine & Ogata 1999; and Wang et al. 2013). During the hydration with water, water initially goes into the inter-aggregate pores which result in starting expansion and leading to a sudden raising in the swelling pressure. By continuing the water-wetting process, the bonds between the structure of the layers weaken which leads to decreasing the swelling pressure and deformation. Finally, because of the high amount of montmorillonite, the swelling characteristic overcomes the collapse of inter-aggregate pores, and hence, the swelling pressure increases again until reaching a constant value. The behavior of swelling evolution observed in the present study is in agreement with some of the previous investigations of swelling pressure of bentonite-based materials, for instance, Wang et al. (2013) conducted a laboratory test on the experimental small-scale test (1/10) with the controlled condition that showed a decrease after reaching the maximum value of swelling pressure in constant-volume condition. The results of this study show the peak swelling pressure increases by increasing the initial dry density which is shown in Figure 6.

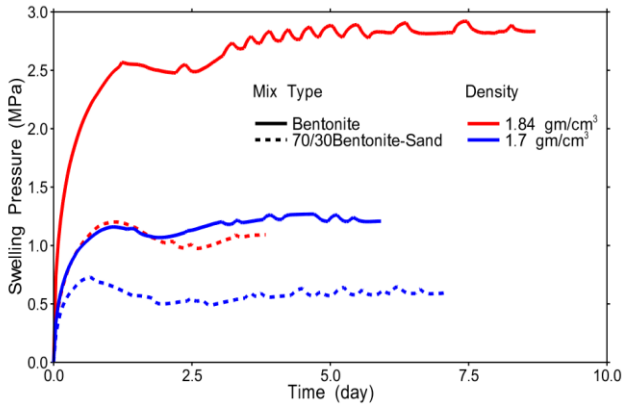

Figure 5. Swelling pressure of pure bentonite and bentonite-sand (70-30) mixtures with different dry densities

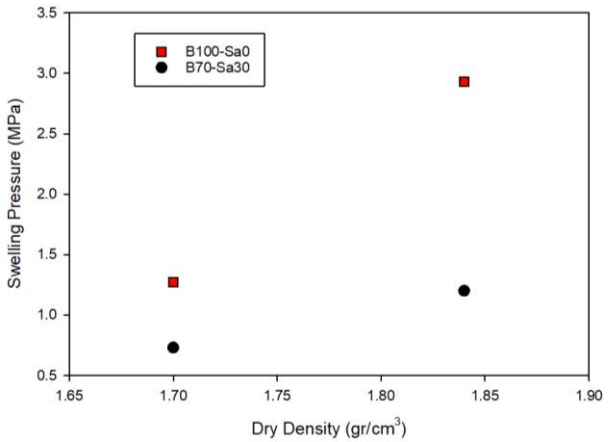

Figure 6. Maximum swelling pressure versus final dry density of pure bentonite and bentonite-sand (70-30) mixtures

Figure 7 shows the variation of swelling pressure versus the final dry density of bentonite obtained in this study and compared with results from other studies(Dixon et al. 1996; Karnland et al. 2007; Karnland et al. 2008; Agus & Schanz 2008; Wang et al. 2012). This study underestimates the swelling pressure compared to other studies as shown in Figure 8. The difference can be attributed to different experimental methods that can affect the swelling pressure. The difference in loading and wetting conditions can result in different values of swelling pressure. Most of the reported CV tests use the common compression load cells for the measurement of swelling pressure. These load cells can cause a major drawback which is related to the induced strain by the swelling of soils. This strain causes significant underestimation, especially when highly expansive soils are tested (Tang et

al. 2011). Furthermore, different pre-treatment related to the preparation of the sample (water content or compaction load) leads to the difference in swelling pressure (Kaufhold et al. 2015). Therefore, the difference between swelling pressures obtained by different investigations is related to the experimental method and the initial condition of preparing samples.

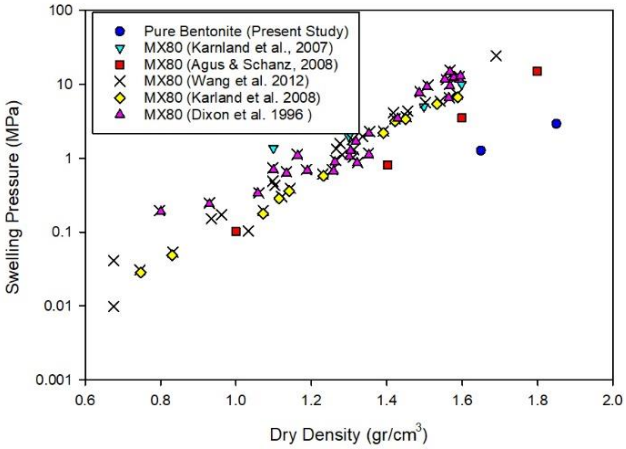

Figure 7. Swelling pressure versus final dry density for different references and the present study

Similar behavior for bentonite mixture with 30-70 sand-bentonite identified which is presented in Figures 5 and 6.

Table 4 listed the value of the peak swelling pressure of different samples.

Table 4. Peak swelling pressure

Test No.	Method	Peak Swelling pressure (MPa)
B70-Sa30-1.70	CV	0.73
B70-Sa30-1.84	CV	1.20
B100-Sa0-1.70	CV	1.27
B100-Sa0-1.84	CV	2.93

4.1.2 Results of Free Swelling (FS) and Free Swell Index Tests

In regards to the FS test conducted on B100-Sa0-1.85 sample, the results show that almost 15 days were required until the specimen reaches the steady-state condition. Wang et al. (2012) conducted the swelling tests in the long duration, from 80 hours to 1 year that showed the steady-state condition occurred in the initial week of tests. Thus, the duration of tests in this study can be justified reaching the equilibrium and ending the test. Figure 8 shows the variation of vertical swelling strain versus time. The vertical swelling reached a maximum increase in height of 1 mm during the test which indicated a vertical strain of 20%.

In this study, the montmorillonite content is not determined. The free swell index test is performed to identify the swelling potential and indirectly estimate the montmorillonite content of the bentonite materials used in this study. This test repeated on two samples that showed an average differential free swelling index of 1578.5 %. The obtained value of the free swelling index confirmed the high swelling potential of bentonite utilized in this study and a potential high montmorillonite content.

4.2 Numerical Results

Figure 8 shows the results of the simulated free swelling test compared with the results of the experimental test. The simulation result is based on fitting the step value (N_s) of each saturation segment. The results show good agreement between the experiment and simulation.

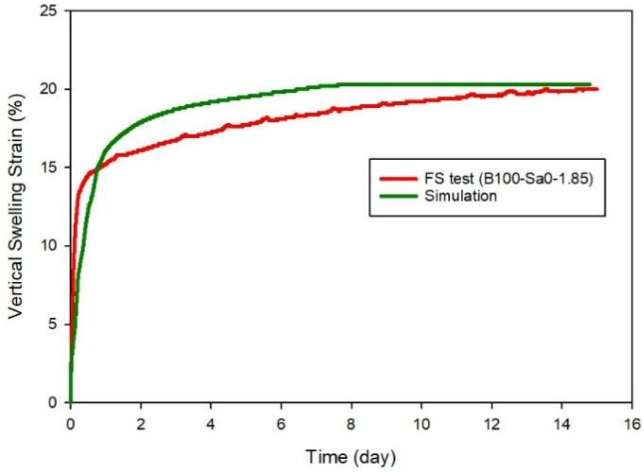

Figure 8. Comparison between experimental and predicted vertical swelling displacement of FS (B100-sa0-1.85)

5 CONCLUSION

The laboratory tests included the constant-volume and the free swelling tests performed to examine the swelling characteristics of bentonite and sand-bentonite mixture. The experiments conducted using a modified triaxial device. As observed, the higher dry density of bentonite-based materials results in the higher swelling pressure. It is suggested that the montmorillonite content of the bentonite evaluate to justify the different results with other works.

A modified constitutive model to predict the evolution of vertical swelling displacement of the free swelling test is used. This model modification overcomes the limitations of FLAC3D swell model, which is the lack in connecting the hydration process and time to the mechanical process. It is recommended that the saturation process and swelling deformation can be linked directly to get more accurate outcomes.

6 REFERENCES

Agus, S.S., and Schanz, T. 2008. A method for predicting swelling pressure of compacted bentonites. *Acta Geotechnica*, 3(2): 125–137. doi:10.1007/s11440-008-0057-0.

ASTM D4546-14. 2014. Standard Test Methods for One-Dimensional Swell or Collapse of Cohesive Soils.

ASTM Book of Standard Specifications, Designation: D (2014): 4546-14.,: 1–9. doi:10.1520/D4546-08.2.

Briggs, S., and Krol, M. 2018. Diffusive Transport Modelling of Corrosion Agents through the Engineered Barrier System in a Deep Geological Repository for Used Nuclear Fuel-*NWMO-TR-2018-06*.

Dixon, D.A., Gray, M.N., and Graham, J. 1996. Swelling and hydraulic properties of bentonites from Japan, Canada and the USA. *Environmental geotechnics*,.

GDS Instruments Ltd. (n.d.). GDS ENTERPRISE LEVEL DYNAMIC TRIAXIAL TESTING SYSTEM Manual.

Itasca Consulting Group. 2011. FLAC V 6.0. fast Lagrangian analysis of continua, user's guide. Minneapolis, *Itasca Consulting Group*.

Jing, L., and Feng, X. 2003. Numerical modeling for coupled thermo-hydro-mechanical and chemical processes (THMC) of geological media - International and Chinese experiences. Yanshilixue Yu Gongcheng Xuebao/*Chinese Journal of Rock Mechanics and Engineering*, **22**(10): 1704–1715.

Karnland, O., and Muurinen, A. 2005. Bentonite swelling pressure in NaCl solutions-Experimentally determined data and model calculations.

Karnland, O., Nilsson, U., Weber, H., and Wersin, P. 2008. Sealing ability of Wyoming bentonite pellets foreseen as buffer material - Laboratory results. *Physics and Chemistry of the Earth*, 33(SUPPL. 1): S472–S475. Elsevier Ltd. doi:10.1016/j.pce.2008.10.024.

Karnland, O., Olsson, S., Nilsson, U., and Sellin, P. 2007. Experimentally determined swelling pressures and geochemical interactions of compacted Wyoming bentonite with highly alkaline solutions. P*hysics and Chemistry of the Earth*, 32(1–7): 275–286. doi:10.1016/j.pce.2006.01.012.

Kaufhold, S., Baille, W., Schanz, T., and Dohrmann, R. 2015. About differences of swelling pressure - dry density relations of compacted bentonites. *Applied Clay Science*, 107: 52–61. Elsevier B.V. doi:10.1016/j.clay.2015.02.002.

Komine, H., and Ogata, N. 1999. Experimental Study on Swelling Characteristics of Sand-Bentonite Mixture For Nuclear Wastw Disposal. *Chemical Pharmaceutical Bulletin*, 17(11): 1460–1462.

Komine, H., Yasuhara, K., and Murakami, S. 2009. Swelling characteristics of bentonites in artificial seawater. *Canadian Geotechnical Journal*, 46(2): 177–189. NRC Research Press.

Millard, A., Mokni, N., Barnichon, J.D., Thatcher, K.E., Bond, A.E., Fraser-Harris, A., Mc Dermott, C., Blaheta, R., Michalec, Z., Hasal, M., Nguyen, T.S., Nasir, O., Fedors, R., Yi, H., and Kolditz, O. 2016. Comparative modelling of laboratory experiments for the hydro-mechanical behaviour of a compacted bentonite–sand mixture. *Environmental Earth Sciences*, 75(19). doi:10.1007/s12665-016-6118-z.

Nasir, O., Calder, N., Walsh, R., Avis, J., Engineering, G., and Kremer, E.P. 2017a. A Concept for Modelling Evolution of Permeability in Re-hydrating Bentonite.

Nasir, O., Nguyen, T.S., Barnichon, J.D., and Millard, A. 2017b. Simulation of hydromechanical behaviour of bentonite seals for containment of radioactive wastes. *Canadian Geotechnical Journ*al, 54(8): 1055–1070. doi:10.1139/cgj-2016-0102.

Noorany, I., Frydman, S., and Detournay, C. 1999. Prediction of soil slope deformation due to wetting. *FLAC and Numerical Modeling in Geomechanics*. pp. 101–108.

OPTA. Bentonite Clay. Available from https://www.optaminerals.com/solutions/construction-products/bentonite-clay/.

Push, P. 1982. Mineral-water interactions and their influence on the physical behaviour of highly compacted Na bentonite. *Canadian Geotechnical Journal*, 19: 381–387.

Sivapullaiah, P. V., Sitharam, T.G., and Subba Rao, K.S. 1987. Modified Free Swell Index for Clays. *Geotechnical Testing Journal*, 10(2): 80–85. doi:10.1520/gtj10936j.

Sun, D., Sun, W., and Fang, L. 2014. Swelling characteristics of Gaomiaozi bentonite and its prediction. *Journal of Rock Mechanics and Geotechnical Engineering*, 6(2): 113–118. doi:10.1016/j.jrmge.2014.01.001.

Sun, D., Zhang, J., Zhang, J., and Zhang, L. 2013. Swelling characteristics of GMZ bentonite and its mixtures with sand.

Sun, D., Zhang, L., Li, J., and Zhang, B. 2015. Evaluation and prediction of the swelling pressures of GMZ bentonites saturated with saline solution.

Tang, C., Tang, A.M., Cui, Y., Delage, P., Laure, E. De, Tang, C., Tang, A.M., Cui, Y., Delage, P., and Schroeder, C. 2011. Investigating the Swelling Pressure of Claystone, Crushed-callovo-oxfordian.

Thatcher, K.E., Bond, A.E., Robinson, P., McDermott, C., Fraser Harris, A.P., and Norris, S. 2016. A new hydro-mechanical model for bentonite resaturation applied to the SEALEX experiments. *Environmental Earth Sciences*, 75(11): 1–17. Springer Berlin Heidelberg. doi:10.1007/s12665-016-5741-z.

Wang, Q., Tang, A.M., Cui, Y.J., Barnichon, J.D., and Ye, W.M. 2013. A comparative study on the hydro-mechanical behavior of compacted bentonite/sand plug based on laboratory and field infiltration tests. *Engineering Geology*, 162: 79–87. doi:10.1016/j.enggeo.2013.05.009.

Wang, Q., Tang, A.M., Cui, Y.J., Delage, P., and Gatmiri, B. 2012. Experimental study on the swelling behaviour of bentonite/claystone mixture. *Engineering Geology*, 124(1): 59–66. Elsevier B.V. doi:10.1016/j.enggeo.2011.10.003.

Zhu, C.M., Ye, W.M., Chen, Y.G., Chen, B., and Cui, Y.J. 2013. Influence of salt solutions on the swelling pressure and hydraulic conductivity of compacted GMZ01 bentonite.